Electronically controlled optical tweezing using space-time-wavelength mapping

Shah Rahman, Rasul Torun, Qiancheng Zhao, Tuva Atasever, and Ozdal Boyraz
EECS Department, University of California – Irvine, CA 92697, USA
oboyraz@uci.edu

ABSTRACT

We propose electronically controlled optical tweezing based on space-time-wavelength mapping technology. By using time-domain modulation, the location and the polarity of force hot-spots created by Lorentz force (gradient force) can be controlled. In this preliminary study we use 150 fs optical pulses that are dispersed in time and space to achieve a focused elliptical beam that is ~20 μm long and ~2 μm wide. We use an electro-optic modulator to modulate power spectral distribution of the femtosecond beam after temporal dispersion and hence change the intensity gradient along the beam at the focal spot. We present a theoretical model, and simulation results from a proposed experimental setup. The results show that we can achieve ±200 pN forces on nano objects (~100 nm) without mechanical beam steering. The intensity of wavelengths along the spectrum can be manipulated by using different RF waveforms to create a desired intensity gradient profile at the focal plane. By choosing the appropriate RF waveform it is possible to create force fields for cell stretching and compression as well as multiple hot spots for attractive or repulsive forces. 2D space-time-wavelength mapping can also be utilized to create tunable 2D force field distribution.

Keywords: optical tweezing, space-time-wavelength mapping, force hot-spots, intensity modulation

1. INTRODUCTION AND RELATED RESEARCH

Acceleration and trapping of organic and inorganic particles using optical forces, a phenomenon referred to as 'optical tweezing', first demonstrated by Ashkin et al. [1], has found a wide range of applications, especially in the biosciences [2–5]. Ashkin's principal breakthrough was in realizing that lasers were capable of producing sufficient irradiances, giving rise to significant optical forces for levitation of small particles against gravity [1], [6]. This concept was applied in building the basis for modern optical trapping technology. An optical trap is formed by tightly focusing a laser beam with an objective lens of high numerical aperture (NA). A dielectric particle near the focus will experience a force due to the transfer of momentum from the scattering of incident photons. The resulting optical force has traditionally been decomposed into two components: (a) a scattering force, in the direction of light propagation and (b) a gradient force, in the direction of the spatial light gradient [7]. Ashkin's seminal work showed that large enough gradient forces could be achieved using a single laser beam, which could overcome the scattering force, and accelerate particles along an intensity gradient. In the Rayleigh scattering regime in particular, the gradient force is more significant and has been utilized to trap sub-wavelength particles. This opened up possibilities of modulating the intensity gradient of a laser beam to manipulate particles, leading to applications in microfluidic systems, cell sorting, and characterization of microorganisms. The traditional approach to intensity modulation involves mechanically steering multiple parallel beams focused onto a narrow region (~50 μm × ~5 μm) to create desired intensity profiles, hence providing control over the gradient force across the region. One example of this is the recent work by Stilgoe and co-workers that demonstrated multiple stable optical traps by steer-controlling the separation between two laser beams [8]. However, these studies fall short of electronic control over optical traps, which offers more flexibility and does not involve bulky moving parts such as beam steering equipment.

Laser Beam Shaping XVI, edited by Andrew Forbes, Todd E. Lizotte, Proc. of SPIE Vol. 9581
95810E · © 2015 SPIE · CCC code: 0277-786X/15/$18 · doi: 10.1117/12.2192487

Downloaded From: http://proceedings.spiedigitallibrary.org/ on 10/17/2015 Terms of Use: http://spiedigitallibrary.org/ss/TermsOfUse.aspx

One established approach toward electronic control involves the use of holographic optical tweezers [9]–[13] where a computer controlled diffractive optical element (DOE) is used to modulate the phase front of a laser beam before feeding it into a conventional tweezer setup. Such techniques typically use liquid crystal spatial light modulators (SLM) to create a pixel array of intended phase shifts which are then imposed on the beam at the corresponding pixels. While HOTs achieve electronic control of optical traps to some extent, it comes at the cost of several drawbacks. Owing to the lack of direct control over the intensity landscape, HOTs produce 'ghost traps' which are undesired intensity peaks (dictated by symmetry conditions) that are strong enough to trap particles [11], [12], [14]. To suppress ghost traps, symmetry of the trapping pattern can be reduced by changing the positions of a few or all the traps as has been shown in [11]. But this approach cannot be applied universally as changing the trapping pattern often leads to loss of functionality.

Furthermore, inhomogeneity among individual optical traps is another limitation of the holographic approach. Curtis and co-workers report an intensity variation among generated traps of higher than 25%, and the figure is greater for higher numbers of traps. This is highly undesirable if a uniform system of traps is required. Curtis *et al* also propose several methods that demonstrate that a trade-off exists between efficiency and uniformity of traps [11]. In addition, a fundamental limitation of HOTs is the confinement of optical traps to discrete spots as opposed to the ability to manipulate an extended continuous intensity landscape [10].

Our novel approach uses space-time-wavelength mapping [15] to achieve a desired spatial intensity gradient at the focal plane and thus provides direct control over the intensity landscape. Through the ability to directly manipulate a continuous landscape, this technique overcomes the limitations of HOTs discussed above, while allowing a greater and direct electronic control of optical traps. Space-time-wavelength mapping also eliminates the issue of unwanted inhomogeneity among produced traps, while not compromising efficiency. Although our theoretical model presented here considers only one dimension, the analysis can be extended to two dimensions using techniques presented in [16] using a virtual imaged phased array (VIPA).

Observing that space-time-wavelength technology has been proven to be useful in arbitrary waveform generation in RF photonics and wide-field real time imaging in microscopy [15], [17], here we take it further and apply it to optical tweezing, incorporating both temporal and spatial modulation of intensity gradient. Preliminary results presented here demonstrate that 20nm wide femtosecond pulses can generate >200pN optical force hot spots whose polarity and location along the focal plane can be controlled to achieve numerous applications such as cell stretching or particle sorting. Electronic tuning allows for greater control over a wider range of achievable force profiles, including producing attractive and repulsive forces between particles at specific spots.

2. MODELING SETUP AND THEORY

We propose a simple experimental setup to demonstrate electronic control of optical tweezing using space-time-wavelength mapping. The setup of our proposed experiment is shown in Fig. 1. A femtosecond laser at 1550 nm with 20 MHz repetition rate, 150 fs pulse-width and 0.5 mW average power propagates through dispersive medium to achieve time wavelength mapping and broaden the pulse-width to 5 ns. An electro-optic modulator adds RF modulation to control the power spectral density profile of the dispersed pulsed laser. To avoid nonlinear distortion, we assume root chirp amplification before space-wavelength mapping through diffraction. An objective lens then focuses the diffracted spectrum onto ~20 μm long and ~2 μm wide elliptical focal spot where each point along the beam is occupied by different wavelengths that arrive at different times due to space-time-wavelength mapping. The intensity of different wavelengths along the spectrum can be manipulated by using different configurations of RF modulation to create a desired intensity gradient at the focal plane. Particles such as polystyrene beads, placed at the focal plane will experience a gradient force from the modulated beam as shown in Fig. 1.

Downloaded From: http://proceedings.spiedigitallibrary.org/ on 10/17/2015 Terms of Use: http://spiedigitallibrary.org/ss/TermsOfUse.aspx

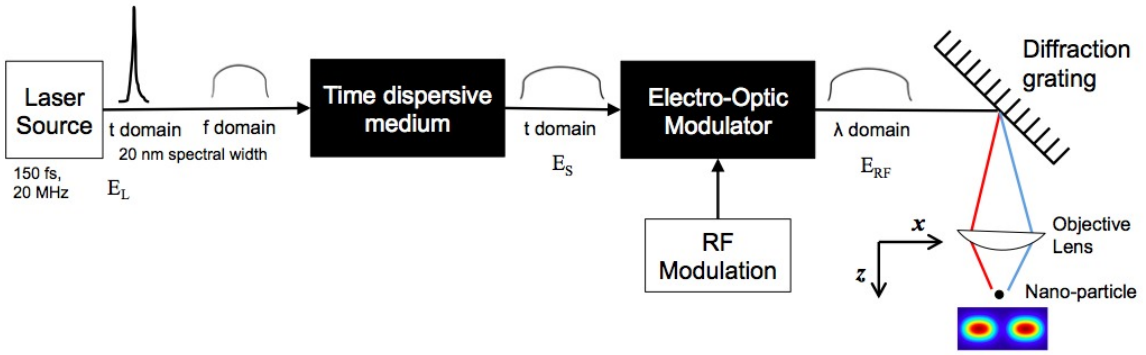

Fig. 1. Proposed experimental setup

We develop a theoretical framework for electronic control of optical force exerted on a particle. We present analytical models for each component shown in the setup in Fig. 1. The theory builds on the gradient force experienced by a particle exposed to a significant intensity gradient. By manipulating the intensity gradient in time and then through space-time-wavelength mapping, it is possible to tweak the optical force to achieve desired force profiles by creating corresponding intensity gradient profiles. This also allows for generation of optical force hot-spots that can be moved along the focal plane. The lateral intensity and force profiles along x do not change drastically along the y direction, and therefore, for simplicity, our analysis here will be confined to the x dimension.

2.1 Space-time-wavelength mapping

Space-time-wavelength (STW) mapping is the result of time-wavelength mapping followed by space-wavelength mapping. A beam comprised of a spectrum of wavelengths is spread out in time by propagating it through time dispersive media. This gives rise to a time-wavelength mapping $\lambda(t)$. Similarly, the beam is made to undergo spatial dispersion causing the wavelengths in the spectrum of the beam to spread out in space, creating a space-wavelength mapping $\lambda(x)$. Through time-domain modulation of the time-dispersed spectrum, we obtain a desired wavelength-dependent intensity profile $I\big(\lambda(t)\big) = I(\lambda)$ for the beam which gets translated into a space-dependent intensity profile $I\big(\lambda(x)\big) = I(x)$ through space-wavelength mapping. Since the gradient force exerted by a beam on a particle is proportional to the intensity gradient [6], STW mapping thus creates a force profile tied to wavelength and space. Our analysis here involves only the lateral force profile at the focal plane (z = 0) and thus we have ignored variation of force in the axial direction. As stated earlier, for further simplicity, we only consider the force along the x-axis (y = 0) on the focal plane.

2.2 Gaussian beam approximation

To assess the force profile, we take Gaussian beam as an example. Assuming the amplitude A_L of the incident field E_L of the femtosecond laser source in Fig. 1. is given by

$$A_L(t) = A_0 \exp\left[-\frac{1}{2}\left(\frac{t}{T_0}\right)^2\right]. \quad (1)$$

Taking a Fourier transform to obtain $A_L(\omega)$, and applying dispersion, the field amplitude $A_S(\omega)$ in the frequency domain is given by

$$A_S(\omega) = A_L(\omega)\exp\left[-\frac{j\beta_2 L\omega^2}{2}\right]. \quad (2)$$

Downloaded From: http://proceedings.spiedigitallibrary.org/ on 10/17/2015 Terms of Use: http://spiedigitallibrary.org/ss/TermsOfUse.aspx

This was followed by inverse Fourier transform to obtain the dispersed field $E_S(t)$ back in time domain as shown in Fig. 2.

Applying chirp and RF modulation $f_{RF}(t)$, the field can be described as

$$E_{RF}(t) = A_S(t)e^{j\omega t}e^{j\phi(t)}f_{RF}(t). \quad (3)$$

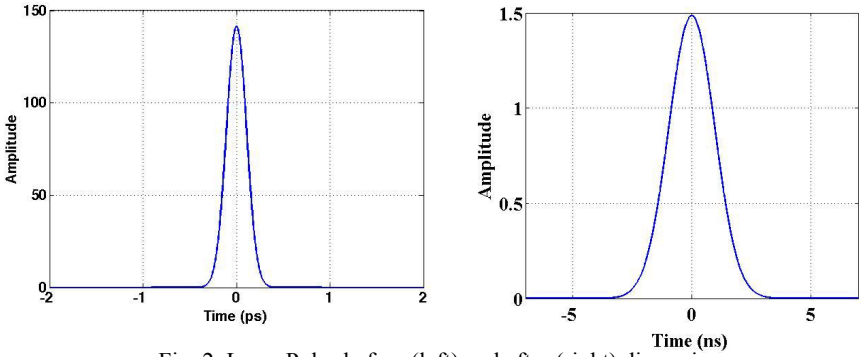

Fig. 2. Laser Pulse before (left) and after (right) dispersion.

Rewriting (3) in terms of a power transfer function instead of field,

$$P_{out}(t) = P_{in}(t){f_{RF}}^2(t) = P_{in}(t)\left[\frac{1}{2} + \frac{1}{2}\cos\left(\frac{\pi}{V_\pi}\left(V_{bias} + v_{RF}(t)\right)\right)\right] \quad (4)$$

where the input power $P_{in}(t) = (A_S(t))^2$, V_π is the half-wave voltage, V_{bias} is the bias voltage, and $v_{RF}(t)$ is the applied RF waveform. One example waveform shown in Fig. 4 is $v_{RF}(t) = \pi e^{-st^{2n}}$ where the integer *n* and the constant *s* can be used to manipulate the shape and width of the RF waveform, and hence the generated force profile.

For a Gaussian beam with a beam size *w*, i.e., the spatial full-width at half maximum, and a focal length *f*, of the Fourier lens shown in Fig. 1., space-wavelength mapping holds that the intensity distribution of focused beams at the image plane is governed by Eq. (5) as given in [17]:

$$I_i(x, \lambda_i) = \frac{P_i}{(f\lambda_i)^2}\exp\left[-\left(\frac{2\pi w(x - x_{pi})}{f\lambda_i}\right)^2\right]. \quad (5)$$

Here, $x_{pi} \approx \frac{G}{\cos(\beta)}f(\lambda_i - \lambda_c) = G_\beta f(\lambda_i - \lambda_c)$ is the relative position of the first order diffraction peak for the wavelength λ_i with respect to the central wavelength λ_c. The $G_\beta = \frac{G}{\cos(\beta)}$ is the effective groov density of the diffraction grating shown in Fig. 1., defined as a function of the first order diffraction angle β. For the beam with wavelength λ, and the incident angle α, the first order diffraction angle β is given by the grating equation $\sin(\alpha) + \sin(\beta) = \lambda G$ which reduces to $2\sin(\beta) = \lambda G$ in a Littrow configuration assumption, where $\alpha = \beta$ [17].

Fig. 3 shows that the force arising from different wavelengths along the spectrum are spatially dispersed and therefore, by tuning the amplitude of individual wavelengths using RF modulation, it is possible to produce intensity profiles for desired spatial force profiles.

Downloaded From: http://proceedings.spiedigitallibrary.org/ on 10/17/2015 Terms of Use: http://spiedigitallibrary.org/ss/TermsOfUse.aspx

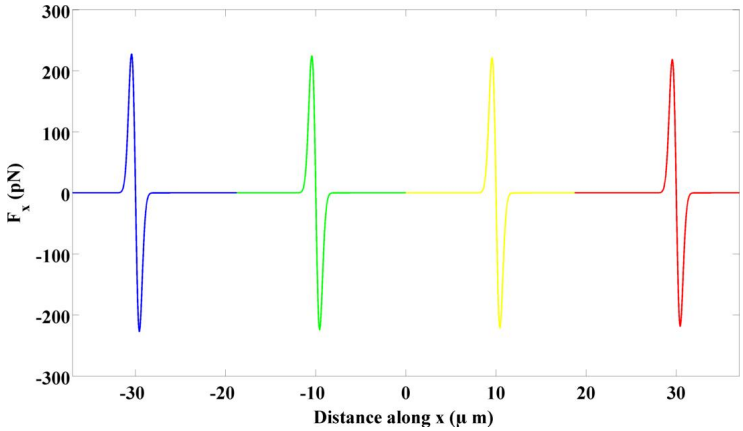

Fig. 3. Force arising from different wavelengths in spectrum.

2.3 Gradient force

To develop a formulation for the optical force at the focal plane, we assume operation under the Rayleigh scattering limit and the dipole approximation. The trapping gradient force from a laser beam on a particle is proportional to the light intensity gradient. The gradient force described in Eqs. (6) and (7) can be derived from the basic formulation of Lorentz force [18].

$$\mathrm{F} = \frac{1}{2}\alpha\nabla\mathrm{E}^2 \tag{6}$$

Incorporating proportionality constants we get,

$$\mathrm{F}(r) = \frac{2\pi n_0 b^3}{c}\left(\frac{m^2-1}{m^2+2}\right)\nabla I(r), \tag{7}$$

where $m = n_1/n_0$ is the relative refractive index of the particle (where n_1 is the refractive index of the particle and n_0 is the refractive index of the surrounding medium), b is the radius of the particle, c is the speed of light, and r is the radial distance from the beam axis.

Taking the gradient of intensity in (5) with respect to the radial distance, we get (8) which gives the intensity gradient of the ith wavelength (λ_i) in the spectrum:

$$\nabla I_i(x) = \frac{\partial I_i(x)}{\partial x} = -\frac{8\pi^2 w^2 (x-x_{pi})}{(f\lambda_i)^4} P_i \exp\left[-\left(\frac{2\pi w(x-x_{pi})}{f\lambda_i}\right)^2\right]. \tag{8}$$

Here we have assumed that we are at the focal plane and that the beam width is the spot size at the focus, *i.e.*, $w = w_0$ for $z = 0$, z being the direction of propagation of the laser. Thus we have not considered a derivative with respect to z in Eq. (8).

Substituting (8) in (7), we get an expression for the optical force dependent on power and radial distance along x of the ith wavelength in the spectrum, as shown in (9):

$$F_i(P_i, \lambda_i, x) = -\frac{16 n_0 w^2 b^3 \pi^3}{c}\left(\frac{m^2-1}{m^2+2}\right)\frac{(x-x_{pi})}{(f\lambda_i)^4} P_i \exp\left[-\left(\frac{2\pi w(x-x_{pi})}{f\lambda_i}\right)^2\right]. \tag{9}$$

Downloaded From: http://proceedings.spiedigitallibrary.org/ on 10/17/2015 Terms of Use: http://spiedigitallibrary.org/ss/TermsOfUse.aspx

Applying a linear superposition on Eq. (9) to get the total force exerted by the entire spectrum, we get,

$$F_{net}(x) = \sum_i F_i(P_i, \lambda_i, x) = -\frac{16 n_0 w^2 \pi^3 b^3}{c}\left(\frac{m^2-1}{m^2+2}\right)\sum_i \frac{(x-x_{pi})}{(f\lambda_i)^4} P_i \exp\left[-\left(\frac{2\pi w(x-x_{pi})}{f\lambda_i}\right)^2\right]. \quad (10)$$

Note that in equations (9) and (10), we have defined the positive x direction to be the direction of positive force. It is important to note here that the power P_i in (10) is controlled by RF modulation.

2.4 Effect of modulation on force profile

Fig. 4 illustrates how RF modulation can be used to generate a desired power profile that can be projected onto an 20 μm strip after diffraction and focusing. The force profile can be plotted using eq. (10) for 100 nm particle radius, as shown in Fig. 4 (right).

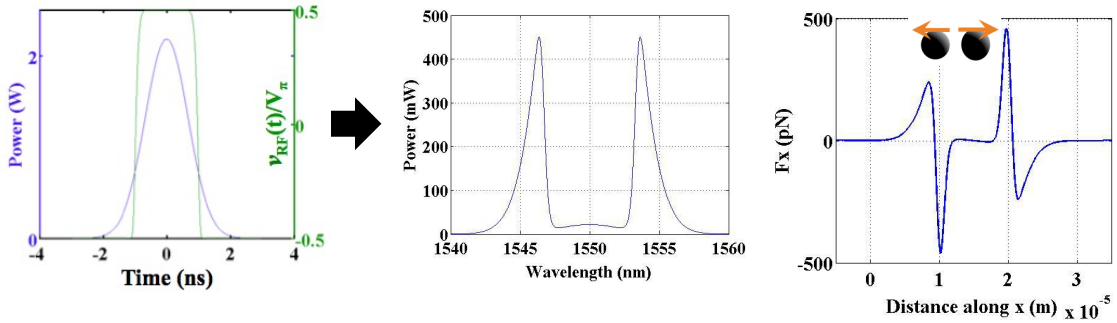

Fig. 4. Normalized RF waveform (left, green), corresponding power profiles (middle), generating desired force profiles

As mentioned earlier, different configurations of RF modulation can be used to manipulate the intensity profile to create hot spots and control their location along the focal plane. Two such results are shown in Fig. 5. Fig. 5a shows the achieved force profile along the spectrum in x domain for two different RF modulation configurations. Fig. 5b shows the modulated power spectral density for the same two configurations. These configurations could be used for cell stretching since the forces achieved at the hot spots (>200pN) are significant. To adjust for cell size, the distance d between the hot spots in Fig. 5a can be controlled using the width τ of the 'well' in the modulated power distribution shown in Fig 5b.

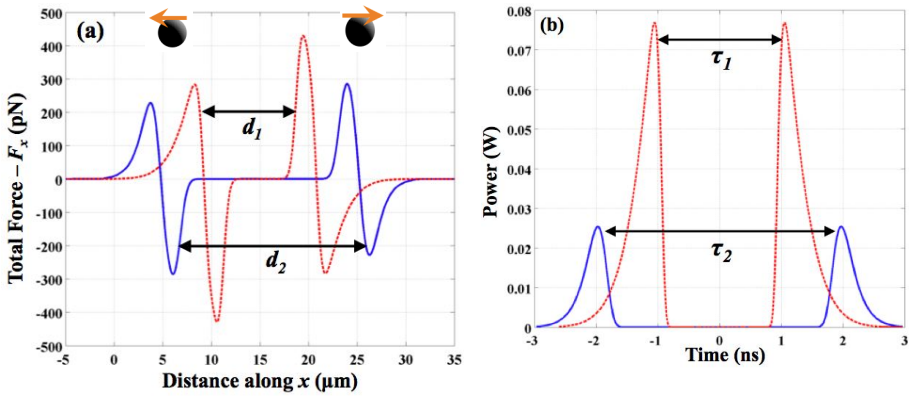

Fig. 5. Simulation results illustrating location control of hotspots. (a) Generated force profile along x, (b) Modulated power

Downloaded From: http://proceedings.spiedigitallibrary.org/ on 10/17/2015 Terms of Use: http://spiedigitallibrary.org/ss/TermsOfUse.aspx

3. SUMMARY

We have presented the idea of achieving desired force profiles in optical tweezing by using space-time-wavelength mapping through electronic tuning, without the need for mechanical beam steering. The significant forces generated using this technique may be put to various applications including stretching, guiding and sorting of micro- and nano-objects. The hot spots created can be used to accelerate particles in a particular direction, and combined with the maneuverability of the spots along the focal plane, it is possible to create more complex scenarios for a wide range of applications, especially in the biosciences. Future work will involve conducting the proposed experiment and corroborating the theory with experimental results.

REFERENCES

[1] A. Ashkin, "Acceleration and Trapping of Particles by Radiation Pressure," *Phys. Rev. Lett.*, vol. 24, no. 4, pp. 156–159, Jan. 1970.

[2] J. Enger, M. Goksör, K. Ramser, P. Hagberg, and D. Hanstorp, "Optical tweezers applied to a microfluidic system," *Lab. Chip*, vol. 4, no. 3, p. 196, 2004.

[3] M. M. Wang, E. Tu, D. E. Raymond, J. M. Yang, H. Zhang, N. Hagen, B. Dees, E. M. Mercer, A. H. Forster, I. Kariv, P. J. Marchand, and W. F. Butler, "Microfluidic sorting of mammalian cells by optical force switching," *Nat. Biotechnol.*, vol. 23, no. 1, pp. 83–87, Jan. 2005.

[4] J. Jass, S. Schedin, E. Fällman, J. Ohlsson, U. J. Nilsson, B. E. Uhlin, and O. Axner, "Physical Properties of Escherichia coli P Pili Measured by Optical Tweezers," *Biophys. J.*, vol. 87, no. 6, pp. 4271–4283, Dec. 2004.

[5] M. P. MacDonald, G. C. Spalding, and K. Dholakia, "Microfluidic sorting in an optical lattice," *Nature*, vol. 426, no. 6965, pp. 421–424, Nov. 2003.

[6] T. A. Nieminen, N. du Preez-Wilkinson, A. B. Stilgoe, V. L. Y. Loke, A. A. M. Bui, and H. Rubinsztein-Dunlop, "Optical tweezers: Theory and modelling," *J. Quant. Spectrosc. Radiat. Transf.*, vol. 146, pp. 59–80, Oct. 2014.

[7] K. C. Neuman and S. M. Block, "Optical trapping," *Rev. Sci. Instrum.*, vol. 75, no. 9, pp. 2787–2809, Sep. 2004.

[8] A. B. Stilgoe, N. R. Heckenberg, T. A. Nieminen, and H. Rubinsztein-Dunlop, "Phase-Transition-like Properties of Double-Beam Optical Tweezers," *Phys. Rev. Lett.*, vol. 107, no. 24, p. 248101, Dec. 2011.

[9] J. E. Curtis, B. A. Koss, and D. G. Grier, "Dynamic holographic optical tweezers," *Opt. Commun.*, vol. 207, no. 1, pp. 169–175, 2002.

[10] D. M. Woerdemann, "Holographic Optical Tweezers," in *Structured Light Fields*, Springer Berlin Heidelberg, 2012, pp. 95–116.

[11] J. E. Curtis, C. H. Schmitz, and J. P. Spatz, "Symmetry dependence of holograms for optical trapping," *Opt. Lett.*, vol. 30, no. 16, pp. 2086–2088, 2005.

Downloaded From: http://proceedings.spiedigitallibrary.org/ on 10/17/2015 Terms of Use: http://spiedigitallibrary.org/ss/TermsOfUse.aspx

[12] M. Polin, K. Ladavac, S.-H. Lee, Y. Roichman, and D. G. Grier, "Optimized holographic optical traps," *Opt. Express*, vol. 13, no. 15, p. 5831, 2005.

[13] M. Montes-Usategui, E. Pleguezuelos, J. Andilla, and E. Martín-Badosa, "Fast generation of holographic optical tweezers by random mask encoding of Fourier components," *Opt. Express*, vol. 14, no. 6, pp. 2101–2107, 2006.

[14] C. Hesseling, M. Woerdemann, A. Hermerschmidt, and C. Denz, "Controlling ghost traps in holographic optical tweezers," *Opt. Lett.*, vol. 36, no. 18, p. 3657, Sep. 2011.

[15] S. K. Kalyoncu, Y. Huang, Q. Song, and O. Boyraz, "Fast Arbitrary Waveform Generation by Using Digital Micromirror Arrays," *IEEE Photonics J.*, vol. 5, no. 1, pp. 5500207–5500207, Feb. 2013.

[16] P. Metz, J. Adam, M. Gerken, and B. Jalali, "Compact, transmissive two-dimensional spatial disperser design with application in simultaneous endoscopic imaging and laser microsurgery," *Appl. Opt.*, vol. 53, no. 3, p. 376, Jan. 2014.

[17] S. K. Kalyoncu, Y. Huang, Q. Song, and O. Boyraz, "Analytical study on arbitrary waveform generation by MEMS micro mirror arrays," *Opt. Express*, vol. 20, no. 25, p. 27542, Dec. 2012.

[18] Y. Harada and T. Asakura, "Radiation forces on a dielectric sphere in the Rayleigh scattering regime," *Opt. Commun.*, vol. 124, no. 5–6, pp. 529–541, Mar. 1996.

Downloaded From: http://proceedings.spiedigitallibrary.org/ on 10/17/2015 Terms of Use: http://spiedigitallibrary.org/ss/TermsOfUse.aspx